Damage threshold influenced by polishing imperfection distribution under 355-nm laser irradiation

Zhen Yu(余振)[1,2], Hong-Ji Qi(齐红基)[1,†], Wei-Li Zhang(张伟丽)[1], Hu Wang(王虎)[1,2], Bin Wang(王斌)[1,2], Yue-Liang Wang(王岳亮)[1,2], and Hao-Peng Huang(黄昊鹏)[1,2]

[1] *Key Laboratory of Materials for High Power Laser, Shanghai Institute of Optics and Fine Mechanics, Shanghai* 201800, *China*
[2] *University of Chinese Academy of Sciences, Beijing* 100049, *China*

(Received 10 March 2017; revised manuscript received 12 May 2017; published online 20 August 2017)

A systematic interpretation of laser-induced damage in the nanosecond regime is realized with a defect distribution buried inside the redeposited layer arising from a polishing process. Under the 355-nm laser irradiation, the size dependence of the defect embedded in the fused silica can be illustrated through the thermal conduction model. Considering CeO_2 as the major initiator, the size distribution with the power law model is determined from the damage probability statistics. To verify the accuracy of the size distribution, the ion output scaling with depth for the inclusion element is obtained with the secondary ion mass spectrometer. For CeO_2 particulates in size of the depth interval with ion output satisfied in the negative exponential form, the corresponding density is consistent with that of the identical size in the calculated size distribution. This coincidence implies an alternative method for the density analysis of photoactive imperfections within optical components at the semi-quantitative level based on the laser damage tests.

Keywords: laser-induced damage, size distribution, photoactive imperfection

PACS: 42.70.Hj, 68.55.Ln, 78.20.nb **DOI:** 10.1088/1674-1056/26/10/104210

1. Introduction

The laser-induced damage of optical components has been the main factor to further improve operation stability, output power, and beam quality in high-power laser systems. The level of current damage resistance for ultraviolet laser irradiation suggests that the extrinsic defects are still the main damage precursors. Previously tremendous researches have revealed that the defects are divided into photoactive imperfections, cracks or scratches, etching residues hidden in the subsurface of optics, which initiate extrinsic damage[1] and material modification[2] in the nanosecond regime. However, the low density of the nanometric imperfections embedded in the subsurface obscures the identification.

To understand the underlying defect characteristics, various statistical models (Dirac,[3] power law,[4] Gaussian law,[5] etc.) of defect ensemble are proposed to fit the experimental damage probability curve. The thermal conduction model is also applied for a given class of defects to correlate the defect size distribution and damage probability curve.[6] Nevertheless, the arbitrarily formed threshold distribution fitting was just purposed to highlight the potential candidates and give a plausible explanation for the real physical meaning. In our essay, the thermal-coupling damage model is expanded to validate the defect ensembles and size distribution buried in the subsurface layer, which suggests an alternate approach to probing the density of photoactive defects.

In this study, a synthetical model is used to identify the size distribution of ceria inclusions embedded in the subsurface of polished fused silica, considering the CeO_2 specie as the major damage initiator. In Subsection 2.1, the threshold versus inclusion size curve is calculated using the thermal conduction equation with the Mie theory. In Subsection 2.2, we investigate the damage probability as a function of defect aggregation population whose threshold is lower than its local fluence in the irradiated area. Assuming the defect density versus size distribution follows a negative power law, the correspondence between the laser fluence and defect size is deduced. In Section 3, the rationality of this methodology is checked by the measurements with a secondary ion mass spectrometer (SIMS) and the further applications are discussed.

2. Model

For the laser-induced damage in the ultraviolet regime, the strong absorption of laser energy for the photo-active defect results in a dramatic temperature increase, melting of the surrounding matrix, phase explosion, and severe surface modification in steps. Especially for thermal-coupling damage, the melting point of the surrounding matrix is usually regarded as the benchmark of damage occurrence.

In the current high-power laser facility, the fused silica substrate serves as the most extensive optical components. Laser damage typically takes place on the rear surface of the fused silica optics.[7] Associated with the polishing process, the CeO_2 particulates are introduced as the composition of

†Corresponding author. E-mail: qhj@siom.ac.cn

© 2017 Chinese Physical Society and IOP Publishing Ltd

the polishing slurry[8] and are regarded as the main damage precursors embedded in the subsurface layer. To verify the methodology of our work, we choose the fused silica substrate as the study object to determine the size distribution of the CeO_2 inclusions.

2.1. Thermal-coupling damage threshold

Under ultraviolet laser irradiation, the absorption parameter of the spherical defect is reckoned with the Mie theory. The power absorbed by a single ceria defect can be calculated using the following description:

$$Q = \alpha I \pi a^2,$$

in which α is the absorption efficiency per unit absorption cross section, I is the laser intensity, and a is the defect radius. Here the refractive index for CeO_2 is $2.0 + 0.20$i in the 355-nm wavelength.[9] The details of this model with Mie theory for the calculation are referred from Gao *et al.*[10] The relation of the absorptivity σ varied with radius a for the CeO_2 particulates surrounded by the fused silica is represented by the black line depicted in Fig. 1.

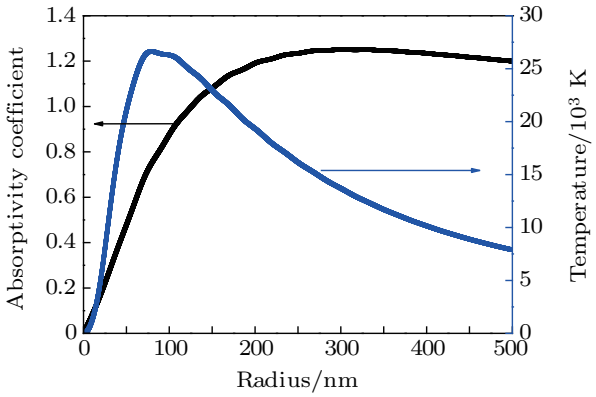


Fig. 1. (color online) The absorptivity coefficient (black line) and temperature (blue line) induced by the 355-nm laser (8 ns, 1.2 J/cm^2) for the CeO_2 particulate of different radius surrounded by the silica matrix.

Since the size of defects is of two orders of magnitude smaller than that of the damage pits, the defect is just treated as the seed for the damage explosion.[11] The various sizes of defects indicate the different laser fluence strengths required to reach the critical point. When the interfacial temperature exceeds the melting point of the surrounding matrix, the optical breakdown is initiated. The melting point of the fused silica sample is usually considered as approximately 2000 K.[12] As the photoactive inclusions are of a higher thermal conductivity than the surrounding matrix, the classical approximation is applied for the uniform temperature distributed throughout the spherical inclusion particulates. In that precondition, the evaluation of temperature inside the core can be attained by solving the heat conduction equation[4]

$$\frac{\partial T}{\partial t} = D_0 \Delta T.$$

The boundary condition ($r = a$) is

$$\alpha I(t) = -4\kappa \frac{\partial T}{\partial r} + \frac{4}{3}\rho C a \frac{\partial T}{\partial t},$$

where D_0 and κ are the thermal diffusivity and conductivity of the surrounding matrix, respectively, and ρ and C are the density and heat capacity of the particle, respectively.

The defects in size around tens of nanometers attract extensive concern due to them being the most vulnerable to initiate surface burns. Figure 1 represents the melting point arrival of the fused silica with a prompt temperature rise in the nanometer-sized region of around 20 nm∼60 nm irradiated by the ultraviolet laser (8 ns, 1.2 mJ/cm^2). For small defects, the high surface-to-volume ratio of such bodies promotes heat loss caused by heat transfer. On the contrary, it becomes more difficult to accumulate sufficient heat to realize the critical temperature in terms of the large inclusions. The defect size is approximately 79 nm at the maximum temperature.

For a given experimental environment of laser damage tests, the minimum fluence that can initiate the laser damage is well known as the critical fluence corresponding to an identical defect size. Combined with the heat conduction equation, the critical fluence (Gaussian, 8 ns, 355 nm) can be calculated as a function of inclusion size. After the fine fabrication process in the fused silica substrate, the large-sized inclusion can be removed while nanoabsorbers remain in the subsurface layer.

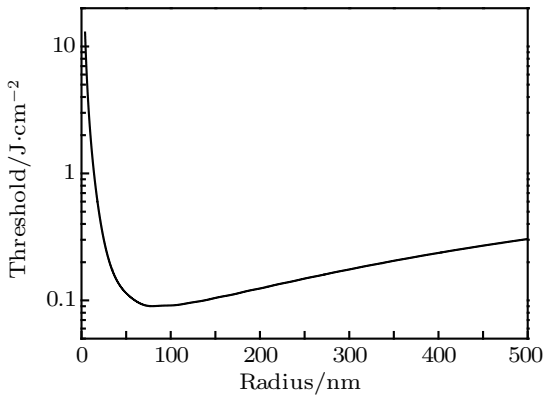


Fig. 2. Calculated threshold curves of critical fluence as a function of fluence (8 ns, 355 nm) in the case of CeO_2 particles buried in fused silica substrate.

Seen from Fig. 2, the critical fluence descends sharply with the defect radius up to 70 nm and then increase slowly since after the turning point. In terms of small defects, the drastic increase of absorptivity coefficient with size contributes to sharp decline of critical fluence in the front part of the curve. In the rear part of the curve, the slow increase of the critical fluence can be interpreted by the toughness of enough heat accumulation for the big volume. The most sensitive size for the lowest damage threshold is 79 nm almost the same as that for the highest temperature arrival in Fig. 1.

2.2. Fitted inclusion density distributed with radius

The laser-induced damage for an identical photo-active inclusion is probabilistic under a specific laser fluence because of the inhomogeneous medium contact and random variation of inclusion spatial occupation.[11] Through the probability statistics method, the damage probability versus the fluence curve is plotted to access the performance of the laser-induced damage resistance. We assume that the probability of damage occurrence will increase with the number of defects under the laser shot. Therefore, the differential function of damage probability $p(S,F)$ versus fluence F corresponds to the increment rate of defect amount under the irradiated area S multiplied by the undamaged probability. The relation can be expressed in the following form:

$$\frac{\partial p(S,F)}{\partial F} = Sn(F)\left(1-p(S,F)\right).$$

Considering the aggregation effect but the additive contribution from the defect coupling on damage initiation, the evaluation methodology serves as the criterion of laser-induced damage probability $p(F)$, given by

$$p(F) = 1-\exp\left(-N(F)\right),$$

where $N(F)$ is the number of defects located under the laser spot of central fluence F, given by

$$N(F) = \int_0^F g(T)S_T(F)\,\mathrm{d}T,$$

where $g(T)$ is the defect density, and $S_T(F)$ is the part of the laser irradiation area with a central fluence F greater than the precursor critical fluence T, described by Krol.[8]

On views of the correlation between laser-induced damage probability curve and defect distribution, a series of optical components are subject to laser irradiation tests to evaluate the internal defect density. If the inclusion is determined as the main type of precursor, the inclusion density inside can be obtained.

For the general optical component irradiated by the laser shot with the central fluence slightly higher than the 0% damage threshold, the damage tends to occur in the spot center. Provided the inclusions disperse with sizes that follow the power-index law surrounded by the silica matrix, the number of identical size a per unit area $n(a)$ can be given by

$$n(a) = \frac{N_0}{a^k} \quad (k>1), \tag{1}$$

where a is the inclusion radius, k is a constant, and N_0 is the inclusion areal density.

There exists a lower limit and an upper limit of sizes corresponding to the sensitive defects that can initiate damage. In this manner, the sum of defects under the laser shot $N(F)$ per unit area can be described by the integration of defect numbers with intermediate size as the following expression

$$N(F) = \int_{a_-}^{a_+} n(a)\,\mathrm{d}a. \tag{2}$$

Under the specific laser shot, the smaller defects are of a higher amount as the product of a higher areal density and a wider irradiation area. In account of less contribution to the sum and difficulty to reach the critical melting point for big-sized inclusions, this relevant upper size limit can be altered by infinity within tolerant errors in accordance with the Weibull model for damage lifetime estimation.[13] For a better understanding of the rationality of that simplification, we introduce the Weibull statistical model with the joint of laser-induced damage probability versus fluence in the nanosecond regime

$$p(F_0) = 1-\exp\left(-c_0 F_0^m \frac{S_{\mathrm{eff}}}{m}\right), \tag{3}$$

where F_0 is the central fluence for a Gaussian laser and S_{eff} is the effective irradiation area as a result of the single pulse energy E divided by F_0. The two unknown parameters C_0 and m are respectively the areal density and a constant, which can be solved through numerical fitting. The damage probability $p(F_0)$ corresponds to the fluence distribution of a Gaussian profile while the damage probability for the flat-top profile is of a simpler form.

The local defect density $c(F)$, derived from Eqs. (1) and (2), can be expressed as follows:

$$c(F) = N_0\frac{a_-^{k-1}}{k-1} = c_0 F^m. \tag{4}$$

The similar form of power index of the middle and right terms is not coincidental for the correspondence between a_- and F, which reflects small defects occupying the main contribution to laser-induced damage. The similarity hints that the inclusion dispersion characteristic can be obtained with a mathematical treatment of the damage probability curve.

For the 1-on-1 laser-induced damage tests conducted on the same batch of samples, the corresponding relation can be deduced, expressed by

$$a_- = BF^{\gamma}, \tag{5}$$

in which

$$\begin{cases} N_0 B^{k-1} = c_0(k-1), \\ m = \gamma(k-1), \end{cases} \tag{6}$$

where B and γ are constants in the premise of previous hypothesis. In this formula, the lower limit a_- is the lowest size of these defects which can initiate damage at the local fluence F. In this way, for identical experimental circumstances the

a_- versus F relation will serve as a guide for the inclusion content inside the optical component as soon as k and N_0 are confirmed.

Therefore, the synthetical model of the theory mentioned above can be verified with the depth distribution of ion output detected on the second ion mass spectrometer. In Section 3, we provide a detailed experimental illustration of the points mentioned above.

3. Laser damage experiments and SIMS detection

A schematic depiction of on-line set-up is shown in Fig. 3 and is designed for laser-induced damage tests on the substrate samples of the silica material. The facility consists of an Nd:YAG laser operating at 355 nm (8-ns pulse duration, 10-Hz pulse rate) through a triple frequency conversion from 1064 nm. The attenuator, composed of a half-wave plate and a polarizer and calibrated by a pyroelectric energy meter before every pulse shot, controls the irradiating laser energy on the sample. The detection of beam profile is determinate once before the damage shots with the beam analyzer. The beam equivalent diameter on the sample is 0.86 mm^2 within a fluctuation of around 1.5% within one thousand shots before our damage tests. The total error of the beam fluence is below 15% due to the coherent addition of energy error, beam profile error, and circumstance instability. The laser-induced damage tests comply with the "1-on-1" mode according to the ISO 21254 standard.[14]

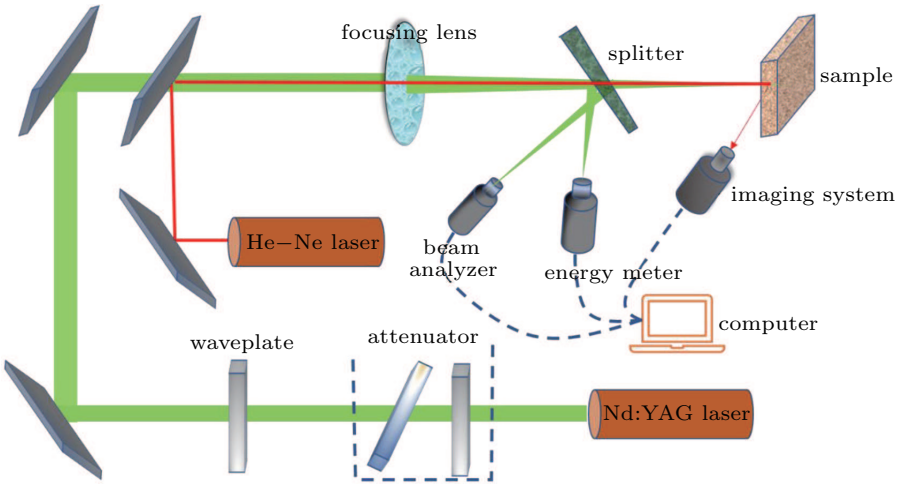


Fig. 3. (color online) Schematic diagram of laser-induced damage testing facility.

The silica wafers (Φ50×5) as the substrate samples are treated with the ultrasonic cleaning to wipe out the surface contaminations. Belonging to the variety of precursors hidden in the subsurface layer, the inclusion particulates have a weaker damage resistance than the scratches and the etching residue. Previous studies have revealed that the ceria particulates surrounded by the silica matrix are vulnerable to be activated by 355-nm laser. In this way, the prominent property of ceria being the photoactive particulate is a good bonding point in which the density of the ceria particulates can be reduced from the damage probability curve. In the experiments, the same batch of six silica wafers is divided equally into two series separately for damage tests and SIMS detection.

3.1. Size distribution extracted from laser damage data

In the damage experiments of the 355-nm laser, the quantitatively similar results are found for the first series of samples. For one sample of the first batch, the fitting curve of damage probability versus fluence is plotted as shown in Fig. 4, with the power-law model.[15] The fitting curve is transferred into the form of the formula (3) to obtain the values (m, c_0), in which $m = 3.2153$ and $c_0 = 0.33863$ mm^{-2}. The 0% damage threshold is around 2.48 J/cm^2, which is obtained from the linear fitted curve and corresponds to the defect size of 8.18 nm in Fig. 2.

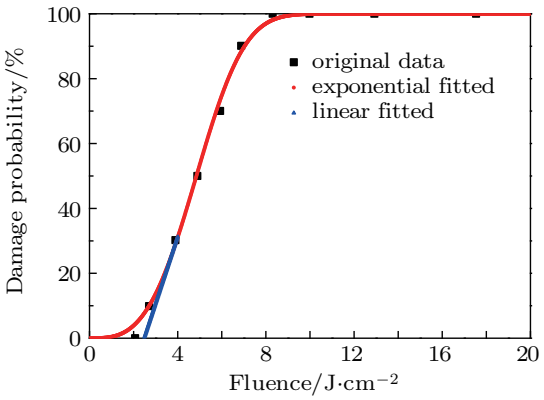


Fig. 4. (color online) Experimental damage probability curve as a function of fluence in the case of the surface of fused silica including inclusion particles.

The resistance performance of the first series against high-power laser irradiation can be estimated with the fitting

parameters m and c_0. The two parameters are separately called the quality factor and defect density coefficient, respectively. In general, the quality factor m characterizes the level of damage initiated by passive defects, and the damage site appears closer to the beam center for a higher m. Meanwhile, the defect density coefficient c_0 corresponds to the probability of damage occurring with a relatively low threshold. The more detailed comparative experiment can be adopted for a thorough discussion in the further study on extrapolated applications.

It has been previously determined that, in general, only small-sized defects are buried inside after refined fabrication of the fused silica substrate. Due to the negligible contribution of large-sized defects, only the radius range below 60 nm is applied to the numerical fitting for formula (5). In Fig. 5, the fitting curve in red matches well with the original one in black, indicating that the small inclusions rather than the large ones are attributed to the damages. The best fit values of B and γ are respectively 14.33 and -0.65.

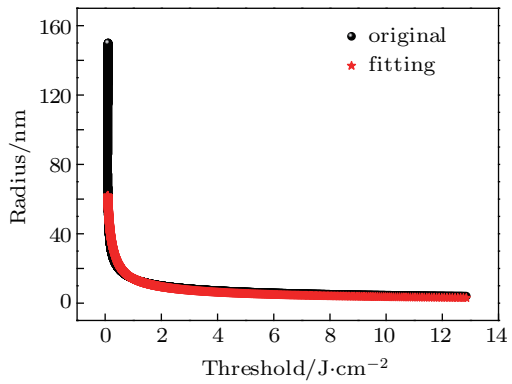


Fig. 5. (color online) Size versus threshold curve (red) fitting with the original in Fig. 2 (black), ruled by Eq. (5) below a radius of 60 nm.

The measurement of inclusion size-distribution is of significant essence to access the material performance such as processing accuracy, laser resistance and attenuation coefficient of optical transmittance. The inclusion particulates, scratches and other imperfections hidden in the subsurface layer can serve as the laser-induced and mechanical damage source.

The details of the damage precursors can promote the comprehension of the subsurface layer. For a clearer picture, the semi-quantitative density of damage precursors can be measured through the extrinsic damage data in our mathematical methodology. To realize that point, the power index k and coefficient N_0 for the defect density distribution should be calculated using Eq. (6). Afterwards, the size distribution of CeO_2 particulates can be attained in Eq. (1).

The distribution of inclusion density with radius presented in Fig. 6, which reflects how the small defect leads to damage occurrence. The density of inclusion with a size of 26 nm is only 0.01 mm^{-2}, leading to the amount less than 0.01 occupied on the laser spot area. It is difficult to initiate the laser-induced damage at such a low density, for which 26 nm is considered as the upper limit of the sensitive sizes. On the contrary, it is tough for defects with a radius below the lower limit of sensitive size a_- to accumulate heat for their high surface-to-volume ratio. In our damage tests, the defect size of 8.18 nm for the 0% damage threshold mentioned above can be regarded as the maximum of the lower limit size a_-.

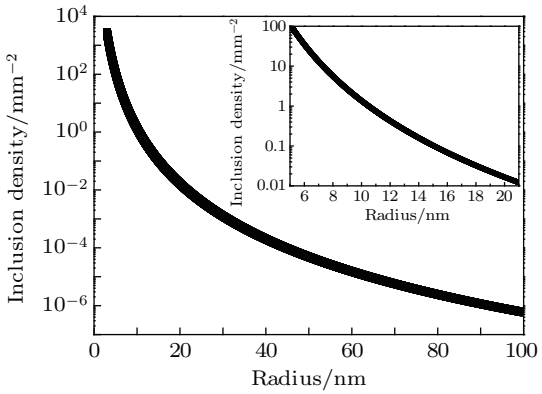


Fig. 6. Density distribution of different sizes extracted from our model for CeO_2 particulates buried in fused silica surface.

It can be assured that the interval (8.18 nm$\sim$ 26 nm) of the inclusion density is reliable directly due to the nature of the extrinsic damage caused by the laser-inclusion interaction. The most sensitive size of defects vulnerable to be laser-ablated perch on not more than tens of nanometers, which agrees with that reported by Kozlowski *et al.*[16] For the verification of the ceria size interval, a SIMS is applied to detect the depth distribution of the inclusion elements.

3.2. SIMS detection

To validate the depth profile of the chemical element composition of impurities embedded in the surface and subsurface layer, a Trift II TOF-SIMS is utilized to monitor the entire mass spectrum with a ppm or ppb detection accuracy level. Before the detection, all the samples were cleaned by the deionized water to remove the surface contaminants from the surrounding environment. The scanning area of test point is 100 μm$\times$100 μm, where a rectangular flat-bottomed pit is caused by the bombardment of Ga ions source on the sample surface with a beam energy of 25 keV. The ion output rate of the impurity element can be converted into a depth distribution in consideration of a stable depth etching rate for the SIMS.

Due to the unrealized calibration for the impurity element, only the relative density can be confirmed from the ion output with the SIMS. The depth distribution of the impurity ion production is illustrated in Fig. 7, whose results are quantitatively similar in the SIMS detection for the other samples.

In Fig. 7, the impurity elements on the subsurface are primarily aluminum, iron and cerium introduced respectively in

the substrate fabrication process, including the cleaning with alumina suspension, grinding of a metal abrasive tool and polishing with ceria burnishing powder. With the comparison of other metal oxide inclusions buried in the fused silica substrate, the ceria particulates are extensively treated as major extrinsic defects with the 355-nm laser irradiation. As observed from Fig. 7, the ion output maintains an approximately negative exponential function with depth between 10 nm for the cerium element. From this point, the maximum size of the ceria particulate is around 10nm on the test area. Consequently, the density of the 10-nm-sized ceria particulates is around 100 mm^{-2} in good accordance with the value in Fig. 6.

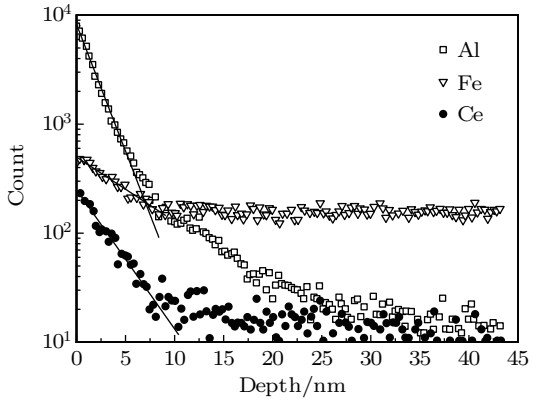


Fig. 7. Depth dependence of product of inclusion ions sputtering in the pit area of 100 μm×100 μm from the TOF-SIMS. The three fitting curves in black represent the negative exponential distribution of the corresponding elements.

4. Conclusion and perspectives

In this study, a synthetical model of the size distribution of inclusion particulate buried in a fused silica substrate has been validated with laser-induced damage tests. The absorptivity coefficient of the ceria particulate surrounded by the fused silica and the assembly effect on the laser-induced damage threshold are determined to evaluate the performance of the damage resistance. The net defect amount under the laser exposure is obtained as the incoherent addition of individual defect numbers of different radii. Therefore, the semi-quantitative density distribution of ceria inclusion is realized with the numerical fitting of the laser-induced damage data. The specific density of the 10nm-sized particulates is verified with the linear interval of the logarithmic ion output with the secondary mass spectroscopy. Furthermore, the model can be modified and developed in extensive appliances for a wider range of optics and can even support a low-cost and indirect irreducible method to probe the density of photo-reactive defects.

References

[1] Miller P E, Suratwala T I, Bude J D, Laurence T A, Shen N, Steele W A, Feit M D, Menapace J A and Wong L L 2010 *Laser Damage Symposium XLI: Annual Symposium on Optical Materials for High Power Lasers*, September 21–23, 2009, Colorado, USA, p. 75040X
[2] Gallais L, Capoulade J, Wagner F, Natoli J Y and Commandre M 2007 *Opt. Commun.* **272** 221
[3] O'Connell and Robert M 1992 *Appl. Opt.* **31** 4143
[4] Feit M D and Rubenchik A M 2004 *XXXV Annual Symposium on Optical Materials for High Power Lasers: Boulder Damage Symposium*, September 20–22, 2003, Colorado, USA, p. 74
[5] Krol H, Gallais L, Grezes-Besset C, Natoli J Y and Commandréa M 2005 *Opt. Commun.* **256** 184
[6] Gallais L, Capoulade J, Natoli J Y and Commandré M 2008 *J. Appl. Phys.* **104** 053120
[7] Liu W W, Wei C Y, Yi K and Shao J D 2015 *Chin. Opt. Lett.* **13** 041407
[8] Dong Z C, Cheng H B, Ye Y and Tam H Y 2014 *Appl. Opt.* **53** 5841
[9] Feit M D, Campbell J H, Faux D R, Genin F R, Kozlowski M R, Rubenchik A M, Riddle R A, Salleo A and Yoshiyama J M 1998 *Laser-induced damage in optical materials*, October 6–8, 1997, Colorado, USA, p. 350
[10] Gao X, Feng G Y, Han J H, Chen N J, T C and Zhou S H 2012 *Appl. Opt.* **51** 2463
[11] Papernov S and Schmid A W 2002 *J. Appl. Phys.* **92** 5720
[12] Bude J, Guss G, Matthews M and Spaeth M L 2007 *Boulder Damage Symposium XXXIX: Annual Symposium on Optical Materials for High Power Lasers*, September 24–26, 2007, Colorado, USA, p. 672009
[13] Negres R A, Liao Z M, Abdulla G M, Cross D A, Norton M A and Carr C W 2011 *Appl. Opt.* **50** D12
[14] ISO21254-1 2011 "Lasers and Laser-Related Equipment–Methods for Laser-Irradiation-Induced Damage Threshold–Part 1: Definitions and General Principles"
[15] Porteus J O and Seitel S C 1984 *Appl. Opt.* **23** 3796
[16] Kozlowski M R, Carr J, Hutcheon I D, Torres R A, Sheehan L M, Camp D W and Yan M 1998 *Laser-Induced Damage in Optical Materials*, October 6–8,1997, Colorado, USA, p. 365